



2017

# Evolution of the Spin Magnetic Moments and Atomic Valence of Vanadium in $VCu_x^+$ , $VAg_x^+$ , and $VAu_x^+$ Clusters ( $x = 3-14$ )

William H. Blades

*Virginia Commonwealth University, University of Virginia*

Arthur C. Reber

*Virginia Commonwealth University*

Shiv N. Khanna

*Virginia Commonwealth University, snkhanna@vcu.edu*

*See next page for additional authors*

Follow this and additional works at: [http://scholarscompass.vcu.edu/phys\\_pubs](http://scholarscompass.vcu.edu/phys_pubs)

 Part of the [Physics Commons](#)

Copyright © 2017 American Chemical Society

Downloaded from

[http://scholarscompass.vcu.edu/phys\\_pubs/208](http://scholarscompass.vcu.edu/phys_pubs/208)

This Article is brought to you for free and open access by the Dept. of Physics at VCU Scholars Compass. It has been accepted for inclusion in Physics Publications by an authorized administrator of VCU Scholars Compass. For more information, please contact [libcompass@vcu.edu](mailto:libcompass@vcu.edu).

---

**Authors**

William H. Blades, Arthur C. Reber, Shiv N. Khanna, Luis López-Sosa, Patrizia Calaminici, and Andreas M. Köster

# Evolution of the Spin Magnetic Moments and Atomic Valence of Vanadium in $\text{VCu}_x^+$ , $\text{VAg}_x^+$ , and $\text{VAu}_x^+$ Clusters ( $x = 3-14$ )

William H. Blades,<sup>†,‡</sup> Arthur C. Reber,<sup>†,‡</sup> Shiv N. Khanna,<sup>\*,†,‡</sup> Luis López-Sosa,<sup>§</sup> Patrizia Calaminici,<sup>\*,§</sup> and Andreas M. Köster<sup>§</sup>

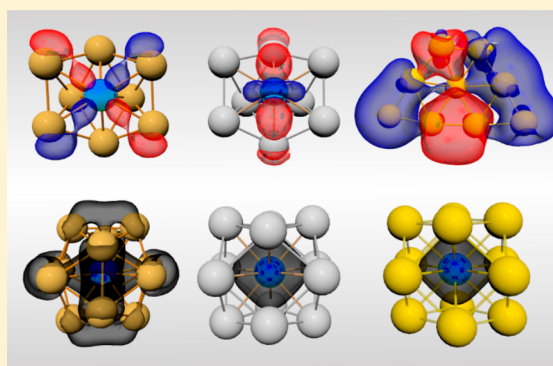
<sup>†</sup>Department of Physics, Virginia Commonwealth University, Richmond, Virginia 23284, United States

<sup>‡</sup>Department of Materials Science and Engineering, University of Virginia, Charlottesville, Virginia 22904, United States

<sup>§</sup>Departamento de Química, CINVESTAV, Av. Instituto Politécnico Nacional 2508, A.P. 14-740, México D.F. 07000, Mexico

## S Supporting Information

**ABSTRACT:** The atomic structures, bonding characteristics, spin magnetic moments, and stability of  $\text{VCu}_x^+$ ,  $\text{VAg}_x^+$ , and  $\text{VAu}_x^+$  ( $x = 3-14$ ) clusters were examined using density functional theory. Our studies indicate that the effective valence of vanadium is size-dependent and that at small sizes some of the valence electrons of vanadium are localized on vanadium, while at larger sizes the 3d orbitals of the vanadium participate in metallic bonding eventually quenching the spin magnetic moment. The electronic stability of the clusters may be understood through a split-shell model that partitions the valence electrons in either a delocalized shell or localized on the vanadium atom. A molecular orbital analysis reveals that in planar clusters the delocalization of the 3d orbital of vanadium is enhanced when surrounded by gold due to enhanced 6s-5d hybridization. Once the clusters become three-dimensional, this hybridization is reduced, and copper most readily delocalizes the vanadium's valence electrons. By understanding these unique features, greater insight is offered into the role of a host material's electronic structure in determining the bonding characteristics and stability of localized spin magnetic moments in quantum confined systems.



## 1. INTRODUCTION

Understanding the manner in which transition-metal impurities with localized spin magnetic moments couple to a nonmagnetic surrounding material is of great importance and has garnered significant attention in recent years.<sup>1-9</sup> Atomic clusters that have a transition metal encapsulated by a nonmagnetic layer are of particular interest due to how drastically the magnetic moment and stability evolve with size, composition, and charge. In small metal clusters, quantum confinement leads to the grouping of electronic states, causing the valence electrons of atomic clusters to form delocalized electronic shells.<sup>10-14</sup> These shells are reminiscent of those found in atoms and have principal and angular momentum quantum numbers that correspond to the electronic configurations  $1S^21P^61D^{10}2S^21F^{14}...$ <sup>15,16</sup> This electronic sequence based on a confined electron gas in a spherical jellium model was proposed by Knight et al., where the ionic charge of the system is distributed uniformly over the size of the cluster.<sup>10</sup> Theoretical and experimental efforts over the past 30 years have shown that clusters with a closed electronic shell exhibit enhanced stability and can be chemically inert.<sup>17-20</sup> Pure copper, silver, and ligated gold clusters follow this conceptual basis, as the valence electrons of each constituent atom

contribute to form the predicted delocalized shells corresponding to this model.<sup>21-26</sup>

However, it has been shown that when a dopant is added to a cluster the valence electrons of that transition-metal impurity will not always participate in bonding with the valence electrons of encapsulating atoms.<sup>3,4,8,27-30</sup> Instead of forming bonding orbitals with the electronic states of the confined nearly free electron gas, the valence electrons of the dopant may remain localized on the atom. This means that the effective valence of a vanadium dopant,  $[\text{Ar}] 3d^34s^2$ , is 2 when only the 4s atomic orbital is involved in bonding, and it becomes 5 when all of the valence electrons participate in bonding. The localized electronic states result in a spin magnetic moment. The spin magnetic moment is size-dependent and is affected by the effective valence of the magnetic dopant. Identifying the cluster size and conditions under which the effective valence of a transition metal changes and begins to bond with the surrounding atoms offers valuable insights into the chemistry of transition-metal defects.

**Received:** February 1, 2017

**Revised:** March 27, 2017

**Published:** March 28, 2017

A magnetic dopant will interact differently depending on the chemical properties of the atoms that surround the dopant. Therefore, by varying the host material, different properties can be realized.<sup>31–34</sup> To this end, we consider the circumstance when a vanadium atom, with an electronic configuration of [Ar] 3d<sup>3</sup>4s<sup>2</sup>, is encapsulated by copper [Ar] 3d<sup>10</sup>4s<sup>1</sup>, silver [Kr] 4d<sup>10</sup>5s<sup>1</sup>, and gold [Xe] 5d<sup>10</sup>6s<sup>1</sup> atoms. While copper, silver, and gold are all group 1B noble metals, they have subtly different electronic structures, which will affect the properties of the clusters. The most significant difference across the 1B series is the degree of hybridization between the s and d valence electrons. Hybridization between two orbitals is maximized when the orbitals have similar energy overlap and spatial overlap. As shown in Figure 1, the energy of the 4s and 3d

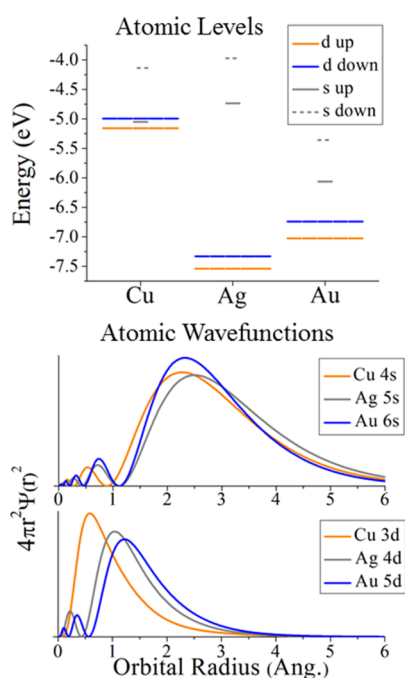


**Figure 1.** Energy levels of the s and d orbitals in a single copper, silver, and gold atom and their respective charge density as a function of orbital radius are shown above. The relativistic effects in gold are responsible for the lowered energy level of the s orbitals and raised d orbitals.

states of the copper are quite similar, suggesting an increased likelihood of hybridization. In silver the 4d orbitals are significantly lower in energy than the 5s orbitals. The 6s and 5d orbitals of gold are not as close in energy as copper but much closer in energy than silver. For reference, the filled 3d orbitals of vanadium lie at  $-5$  eV, and the 4s orbital of V lies at  $-4.6$  eV. The orbital radii of copper, silver, and gold are also shown in Figure 1. The relativistic quantum chemical effects of gold result in the contraction of the 6s orbital and an expansion in the radius of the 5d orbital.<sup>35–38</sup> Figure 1 shows that the 6s orbital of Au is contracted to a shorter radius than that of Ag, while the 5d orbital of Au has a larger radius than Ag. For reference, the maximum for the 4s orbital of vanadium is at 2.82 Å, and the maximum for the 3d orbital of vanadium is at 0.81 Å. For two orbitals to hybridize, they should overlap both in energy and space, and the 6s and 5d orbitals of Au have reasonable overlap in both energy and space. For copper, the 3d orbitals are much more localized than the 4d and 5d orbitals of Ag and Au, so while the energy overlap between the 4s and

3d orbitals of Cu are excellent, the spatial overlap is poor. Because of the combined overlap in both space and energy, small Au clusters tend to have enhanced hybridization between the 6s and 5d orbitals, resulting in unusual properties such as their tendency to form planar structures. These variations in the hybridization of copper, silver, and gold will have an effect on how easily they form bonding orbitals with a transition-metal impurity.

In this study, we identified the lowest ground-state structures and spin magnetic moments of  $\text{VCu}_x^+$ ,  $\text{VAg}_x^+$ , and  $\text{VAu}_x^+$ . The purpose of this work is to determine the size at which the bonding between vanadium atom and copper, silver, and gold begins to occur, what is the size dependence of the effective valence of vanadium, and at what size has the magnetic moment been quenched? At small sizes, a two- to three-dimensional transition is observed, which affects the electronic structure and spin magnetic moment of the cluster. Our calculations also reveal that the enhanced sd hybridization experienced by the gold atoms allows the 1D delocalized shell to begin to fill at smaller size, which provides a lowered alternating spin magnetic moment due to even/odd number of electrons. As the clusters grow in size, the 3d vanadium states start to participate in metallic bonding with the surrounding atoms, and the spin moment begins to systemically decrease at  $\text{VCu}_8^+$ ,  $\text{VAg}_{12}^+$ , and  $\text{VAu}_{11}^+$ , respectively. By using molecular orbital analysis, a detailed evaluation of the electronic profile of each cluster is offered. Enhanced electronic stability is found when there are 6, 8, and 18 delocalized electrons, which corresponds to a filled shell and agrees with a simple shell model. This study helps to clarify the role of the electronic profile of the host material in determining bonding characteristics and stability of localized spin magnetic moments in quantum confined systems.

## 2. THEORETICAL METHODS

Theoretical studies of the electronic structure and ground-state geometries of  $\text{VCu}_x^+$ ,  $\text{VAg}_x^+$ , and  $\text{VAu}_x^+$  were performed using a first-principles density functional theory approach. The calculations were performed using the Amsterdam Density Functional (ADF) set of codes, which uses a linear combination of Slater-type orbitals located at atomic sites, which are represented by the TZ2P basis set.<sup>39</sup> The exchange correlation effects are incorporated via the PBE gradient correct functional.<sup>40</sup> The Zeroth Order Regular Approximation managed the relativistic effects of our system. The lowest-energy structures of  $\text{VCu}_x^+$  and  $\text{VAg}_x^+$  clusters were optimized with the deMon2k code.<sup>41</sup> Details for these calculations were already presented in ref 3 for the  $\text{VAg}_x^+$  clusters. In short, the PW86 exchange and correlation functional was employed for the  $\text{VCu}_x^+$  clusters.<sup>42</sup> The V and Cu atoms were described with DZVP basis sets optimized for generalized gradient approximation.<sup>43</sup> The initial structures for the full geometry optimizations were taken from Born–Oppenheimer molecular dynamics (BOMD) trajectories, which were recorded at 1500 K with a total length of 30 ps. The average temperature in these simulations was controlled with a Nosé–Hoover chain thermostat.<sup>44–46</sup> In this way several hundred structures were optimized to fully explore the potential energy surfaces of these systems. The ground-state atomic configurations were, therefore, determined by starting from several initial configurations and optimizing the geometries by allowing full vibrational freedom without any constraints. In each case, different spin

multiplicities were investigated to find the ground-state spin configuration.

As the cluster size increases, the 3d localized states of V begin to hybridize with the delocalized 1D orbitals of the confined nearly free electron gas to form delocalized orbitals. One of the effects of delocalization is a reduction in exchange splitting. As we will discuss later, we performed a Symmetrized Fragment Orbitals (SFO) analysis, as implemented in the ADF code, to examine the delocalization of the 3d orbitals of V.

### 3. RESULTS AND DISCUSSION

#### 3.1. Structures of $\text{VCu}_x^+$ , $\text{VAg}_x^+$ , and $\text{VAu}_x^+$ Clusters.

We first determined the ground-state structures of  $\text{VM}_x^+$  clusters,  $x = 3-14$ ,  $M = \text{Cu, Ag, and Au}$ . The lowest ground-state structures are shown in Figure 2. Our calculations found that at small sizes  $\text{VCu}_x^+$  prefers three-dimensional geometries, while  $\text{VAg}_x^+$  and  $\text{VAu}_x^+$  favor planar structures.  $\text{VCu}_x^+$  continues to favor a three-dimensional geometry at larger sizes, whereas  $\text{VAg}_x^+$  and  $\text{VAu}_x^+$  undergo a transition from two to three dimensions at  $x = 7$ . The gold vanadium clusters experience another geometric transition. A distorted planar structure is found for  $\text{VAu}_8^+$ , and as a ninth gold atom is added there is a final transition back to a three-dimensional structure at  $\text{VAu}_9^+$ . This result is consistent with the well-known tendency of gold to form planar clusters.<sup>36,47,48</sup> These structural variations have an enormous influence on the bonding characteristics of these small clusters.

**3.2. Multiplicities and Electronic Structure.** Figure 3 displays the multiplicities and electronic shell fillings of the clusters. As already described for the  $\text{VAg}_x^+$  clusters<sup>3</sup> the vanadium atom can possess a  $4s^23d^3$  or  $4s^13d^4$  configuration in these clusters. For the small  $\text{VCu}_x^+$  and  $\text{VAg}_x^+$  clusters until  $x = 7$  the change in the vanadium atom configuration determines the alternating multiplicity of 4 and 5 of the clusters. At  $\text{VCu}_7^+$  and  $\text{VAg}_7^+$  a  $1S^21P^6$  closed-shell electron gas configuration is reached. From here on the  $\text{VCu}_x^+$  and  $\text{VAg}_x^+$  clusters follow different orbital-filling routes. Whereas in  $\text{VCu}_8^+$  a localized 3d orbital of the vanadium atom contributes to the electron gas of the cluster giving rise to a  $1S^21P^61D^2$  electron gas configuration (see Figure 3) and a quenched triplet multiplicity, the separation between the localized 3d vanadium orbitals and the cluster orbitals remains in  $\text{VAg}_8^+$ . As a consequence,  $\text{VAg}_8^+$  possesses a quintet multiplicity due to the  $3d^4$  configuration of the vanadium atom and a  $1S^21P^6$  electron gas configuration.

For the small  $\text{VAu}_x^+$  clusters the situation is very different. In these clusters the vanadium atom only possesses a  $3d^4$  configuration in the case of  $\text{VAu}_2^+$ . From  $\text{VAu}_3^+$  on the multiplicity alternates between 3 and 4. As can be seen from Figure 3 the 1D cluster orbitals are already occupied in  $\text{VAu}_6^+$ , whereas their occupation starts in  $\text{VCu}_x^+$  at  $x = 8$  and in  $\text{VAg}_x^+$  at  $x = 9$ . Note that the filling of the 1D cluster orbitals is interrupted in the gold clusters at  $\text{VAu}_7^+$ . This is due to the  $1S^21P^6$  shell closing in this cluster. In fact, all studied  $\text{VM}_7^+$  ( $M = \text{Cu, Ag, Au}$ ) clusters have the same multiplicity and orbital filling. This underlines the importance of electron gas shell closing in these clusters. While metallic bonding first appears between gold and vanadium, the 3d vanadium electrons are all participating in bonding in  $\text{VCu}_{11}^+$ , while this occurs in  $\text{VAg}_{12}^+$  and  $\text{VAu}_{13}^+$ . As a result, a more or less continuous quenching of the cluster spin multiplicity is observed for these larger clusters with growing cluster size. In conclusion, we find that the vanadium 3d orbitals first become delocalized when interacting

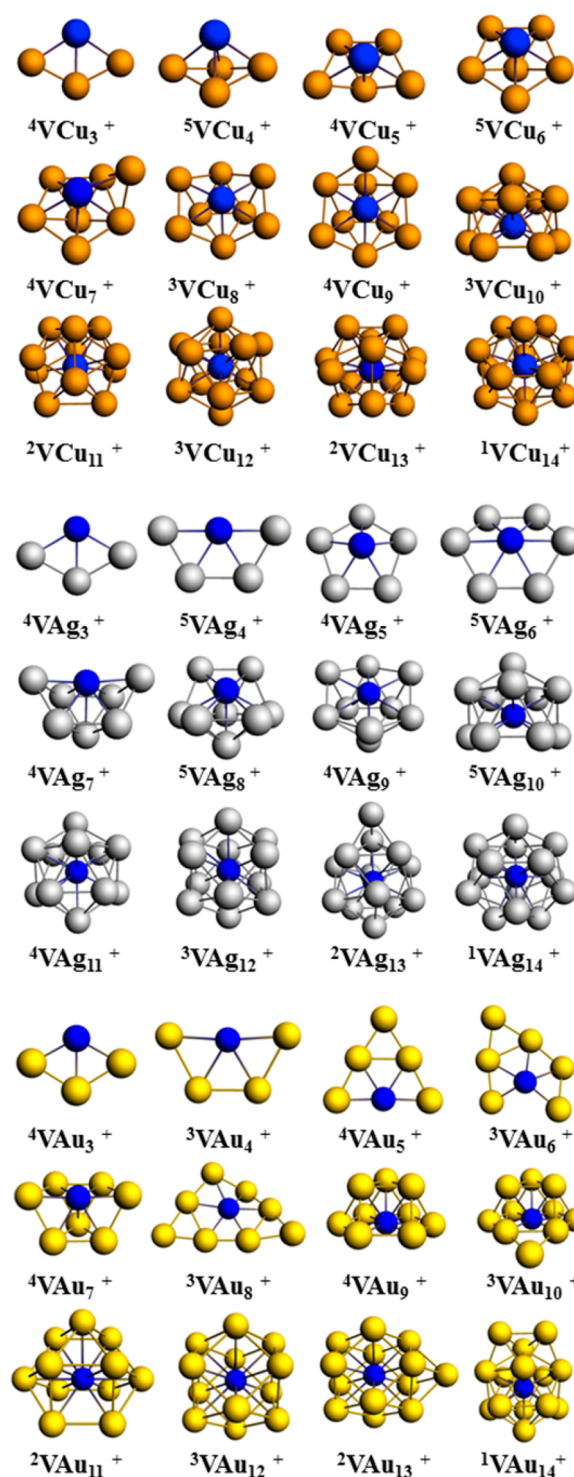
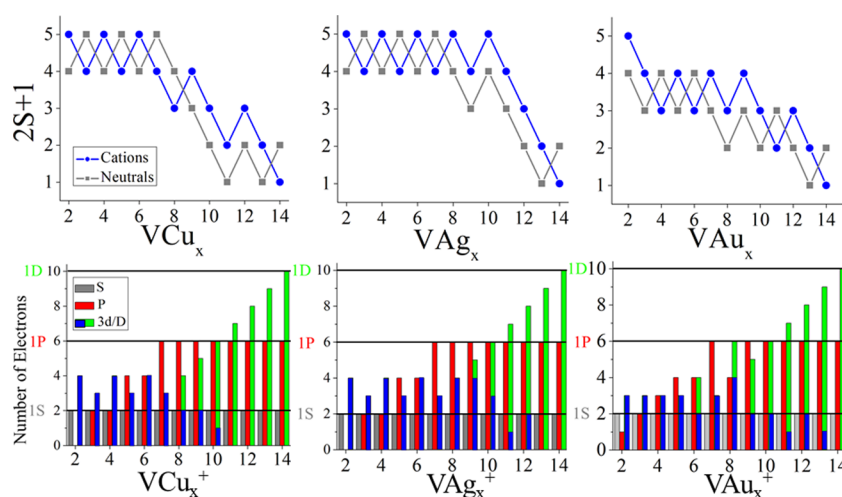


Figure 2. Ground-state geometries and associated spin multiplicities of  $\text{VCu}_x^+$ ,  $\text{VAg}_x^+$ , and  $\text{VAu}_x^+$  ( $x = 3-14$ ).

with gold but first fully participate in the cluster electron gas when interacting with copper.

**3.3. Electronic Properties.** To understand how these electronic structure effects influence the stability of our systems, we examined the highest occupied molecular orbital–lowest unoccupied molecular orbital (HOMO–LUMO) gaps and ionization potentials in Figure 4. We focus on shell, subshell, and partial shell closures that correspond to relatively large gaps and lower ionization potentials. The largest HOMO–LUMO



**Figure 3.** Spin multiplicities (top) and electronic shell fillings (bottom) for  $\text{VCu}_x^+$ ,  $\text{VAg}_x^+$ , and  $\text{VAu}_x^+$ ,  $x = 2-14$ . For comparison the multiplicities of the neutral clusters are also shown. The gray, red, and green columns in the electron shell-filling diagrams represent the occupation of the 1S, 1P, and 1D shells, respectively. The occupation of the localized 3d vanadium orbitals is given by the blue columns that are added to the green 1D column.

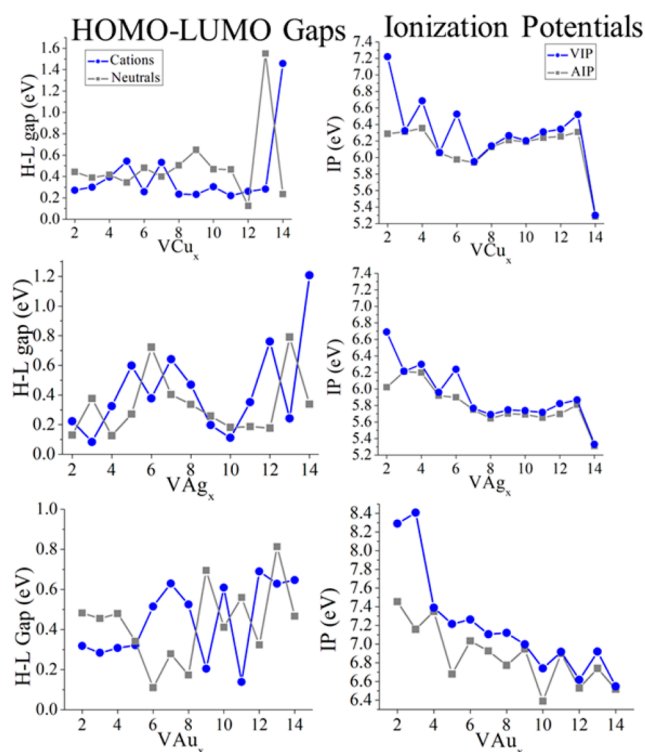


**Figure 4.** HOMO–LUMO gaps of  $\text{VCu}_x^+$ ,  $\text{VAg}_x^+$ , and  $\text{VAu}_x^+$  ( $x = 2-14$ ) as well as the ionization potentials, vertical and adiabatic, of the corresponding neutral clusters. The gaps for nonsinglet species are for any spin.

gaps are observed for  $\text{VCu}_{14}^+$  and  $\text{VAg}_{14}^+$ , which correspond to clusters with 18 valence electrons, consistent with a closed electronic shell  $1S^21P^61D^{10}$  cluster orbital occupation, where all five vanadium electrons are participating in bonding. Note that  $\text{VAu}_{14}^+$  has a HOMO–LUMO gap that is significantly smaller than those for Cu and Ag. This low HOMO–LUMO gap can be attributed to the relatively unsymmetrical geometric configuration, which lowers the LUMO atomic  $3d_z^2$  orbital shown in Figure 7. Peaks in the HOMO–LUMO gap are also found for  $\text{VCu}_7^+$ ,  $\text{VAg}_7^+$ , and  $\text{VAu}_7^+$ . These clusters are all three-dimensional, and their enhanced electronic stability is due

to their delocalized electrons having eight valence electrons with a closed electronic shell while having three localized electrons on the V atom. The  $1S^2$ ,  $1P_x^2$ ,  $1P_y^2$ , and  $1P_z^2$  orbitals are filled resulting in an electronic structure of  $1S^21P^63d^3$ , implying that the effective valence of vanadium is 2 at this size. A partial shell closure corresponding to local maxima in HOMO–LUMO gaps of 0.54 and 0.60 eV is found for  ${}^4\text{VCu}_5^+$  and  ${}^4\text{VAg}_5^+$ , respectively. Both clusters have six delocalized electrons providing similar electronic structures of  $1S^21P_x^21P_y^23d^3$ , and their respective geometries are distinctively planar or oblate.  ${}^4\text{VCu}_5^+$  has a three-dimensional oblate structure, while  ${}^4\text{VAg}_5^+$  favors a quasi-planar structure. In both cases, the vanadium atom's 4s electrons participate in the delocalized electronic shells via metallic bonding, and there are three localized 3d electrons. The delocalized electron cloud provides enhanced electronic stability due to its closed-shell nature, as clusters with planar or oblate structures have magic numbers that are two less than the usual magic number. The electronic structure may be described as  $1S^21P^43d^3$ . This partial shell closure is also observed in  ${}^4\text{VAu}_5^+$ , which has a planar structure and has its  $1S^2$ ,  $1P_x^2$ , and  $1P_y^2$  orbitals filled. However, our calculations reveal that the HOMO is raised in energy, providing large exchange splitting and a lowered gap of only 0.32 eV. This gap is relatively small compared to the copper and silver counterparts and does not lead to enhanced stability.

A molecular orbital analysis is used to understand the evolution of the electronic structure of the transition-metal doped noble-metal clusters. This provides insight into how the electronic structure of the vanadium atom changes the bonding characteristics and structure of the copper, silver, and gold, respectively. When the vanadium atom is introduced into the copper, silver, and gold clusters, respectively, the 4s electrons of the vanadium atom will initially participate in the metallic bonding with the cluster orbitals of the surrounding metal atoms. Until the cluster grows in size, the vanadium 3d electrons will remain localized on the vanadium site, contributing a spin magnetic moment. In this context, we define a localized orbital as having a vanadium 3d orbital contribution of 50% or more using the gross SFO population. Exactly when the 3d electrons of the vanadium start to join the metallic bonding of the surrounding metal atoms depends on

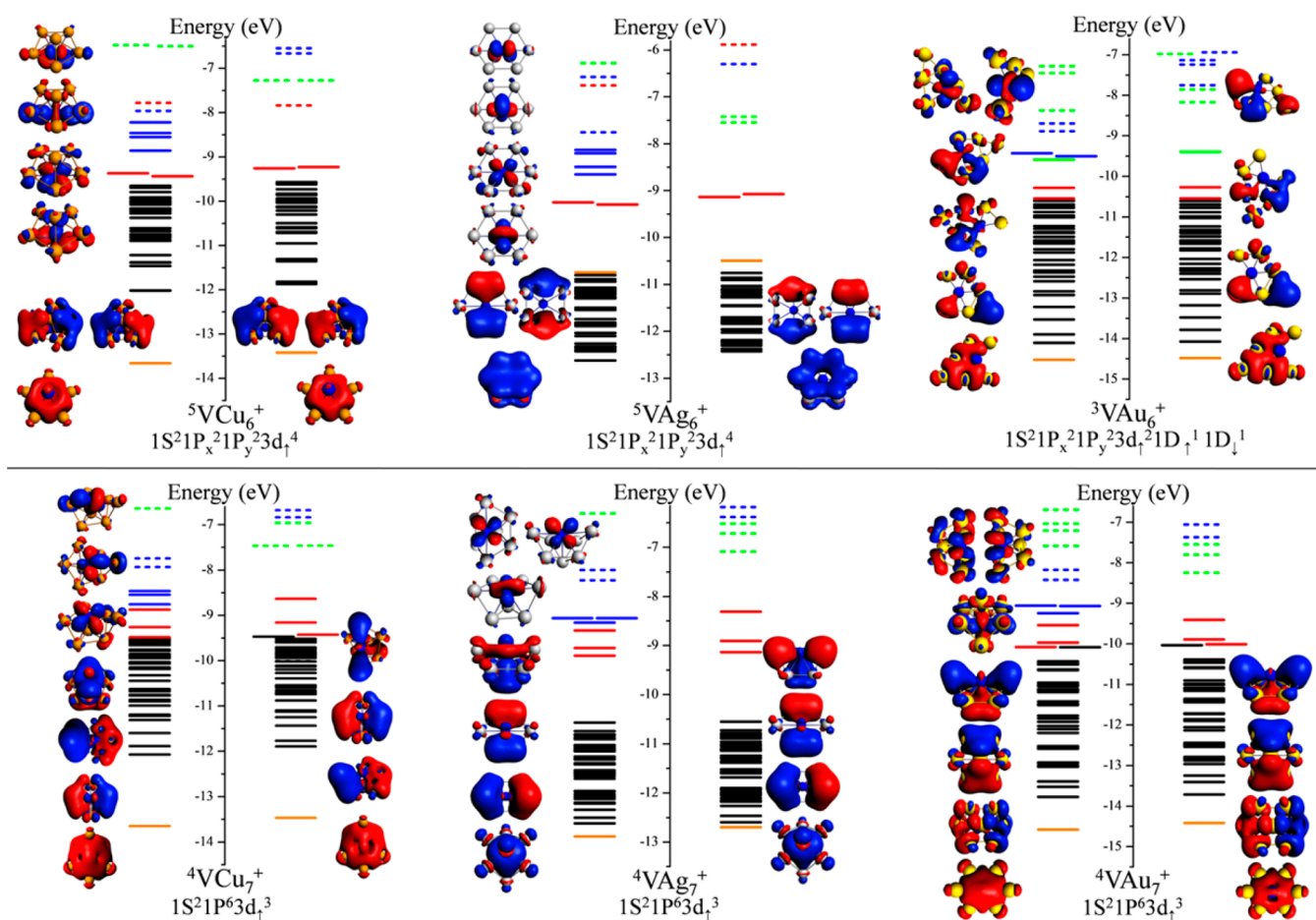


**Figure 5.** Molecular orbital diagrams for  $\text{VCu}_x^+$ ,  $\text{VAg}_x^+$ , and  $\text{VAu}_x^+$  ( $x = 6-7$ ). The filled orange, red, and green lines represent orbitals corresponding to the 1S, 1P, and 1D shells, respectively, and the blue lines represent the localized 3d vanadium orbitals. The dashed lines, the color of which represents the same orbitals as the filled lines, denote the unoccupied orbitals. Pictures of the delocalized orbitals and the localized 3d vanadium orbitals are stacked, as they appear in the molecular orbital analysis.

the electronic structure of the cluster and the subsequent geometry it provides.

**3.4. Two- to Three-Dimensional Transition,  $\text{VM}_x^+$ ,  $x = 4-9$ ,  $M = \text{Cu, Ag, and Au}$ .** One of the more interesting features of these bimetallic metal clusters is the transition from two- to three-dimensional structures. While small  $\text{VCu}_x^+$  clusters prefer three-dimensional geometries, our calculations show that  $\text{VAg}_x^+$  and  $\text{VAu}_x^+$  favor planar structures. To highlight this, the molecular orbital diagrams of  $x = 6-9$  are shown in Figures 5 and 6. The electronic structure of  ${}^5\text{VCu}_6^+$  has the  $1\text{S}^2$ ,  $1\text{P}_x^2$ , and  $1\text{P}_y^2$  cluster orbitals filled; however, instead of filling the  $1\text{P}_z^2$  orbital the vanadium atom is providing four localized 3d electrons in the spin-majority channel. These four localized electrons are responsible for the large exchange splitting observed in the electronic profile and a lowered HOMO–LUMO gap.  ${}^4\text{VCu}_7^+$  has a prolate three-dimensional geometry, which accounts for the relatively large  $1\text{P}^6$  orbital width. The vanadium atom is contributing three localized 3d electrons to the majority-spin channel, and the  $1\text{S}^2$ ,  $1\text{P}_x^2$ ,  $1\text{P}_y^2$ , and  $1\text{P}_z^2$  orbitals are filled resulting in an electronic structure of  $1\text{S}^2 1\text{P}^6 3\text{d}^3$ . The filling of the  $1\text{S}^2$  and  $1\text{P}^6$  orbitals corresponds to eight delocalized electrons, allowing for a full shell closure, and enhanced stability. At  ${}^3\text{VCu}_8^+$  both the  $1\text{S}^2$  and  $1\text{P}^6$  shells are filled. As the molecular orbital diagrams reveal in Figure 6, an additional  $1\text{D}^2$  occupation is found. This lowers the

magnetic moment to 2 and yields an electronic structure of  $1\text{S}^2 1\text{P}^6 1\text{D}^2 3\text{d}^2$ .

${}^5\text{VAg}_6^+$  has a distorted planar geometry. The vanadium atom is providing four localized 3d electrons in the spin-majority channel, as the  $1\text{P}_z^2$  delocalized orbital is still too high in energy to be filled. This is responsible for a spin magnetic moment of four and substantial exchange splitting. The distorted planar geometry of  ${}^3\text{VAu}_6^+$  has the  $1\text{S}^2$ ,  $1\text{P}_x^2$ , and  $1\text{P}_y^2$  orbitals filled as well; however, the vanadium atom is only providing two localized 3d electrons to the majority-spin channel. The other 3d electron is participating in metallic bonding with the gold atoms and contributing to the 1D cluster orbital in the spin majority and minority channels. The 1D orbital of  $\text{VAu}_6^+$  has less than a 15% orbital contribution from the V 3d orbitals, clearly marking it as delocalized. The formation of these delocalized orbitals shows that the bonding between gold and vanadium occurs more readily than in copper or silver, in this size regime. For the sake of comparison, this enhanced bonding is also observed for the three-dimensional structure of  $\text{VAu}_6^+$ . However, the two-dimensional structure of  ${}^3\text{VAu}_6^+$  is 0.32 eV more stable than the most stable three-dimensional one, making the planar geometry the preferred configuration. As the clusters grow in size, the two- to three-dimensional geometric transition undertaken by the silver and gold vanadium clusters occurs at  $\text{VAg}_7^+$  and  $\text{VAu}_7^+$  when there are eight delocalized electrons. Our calculations reveal that the three-dimensional

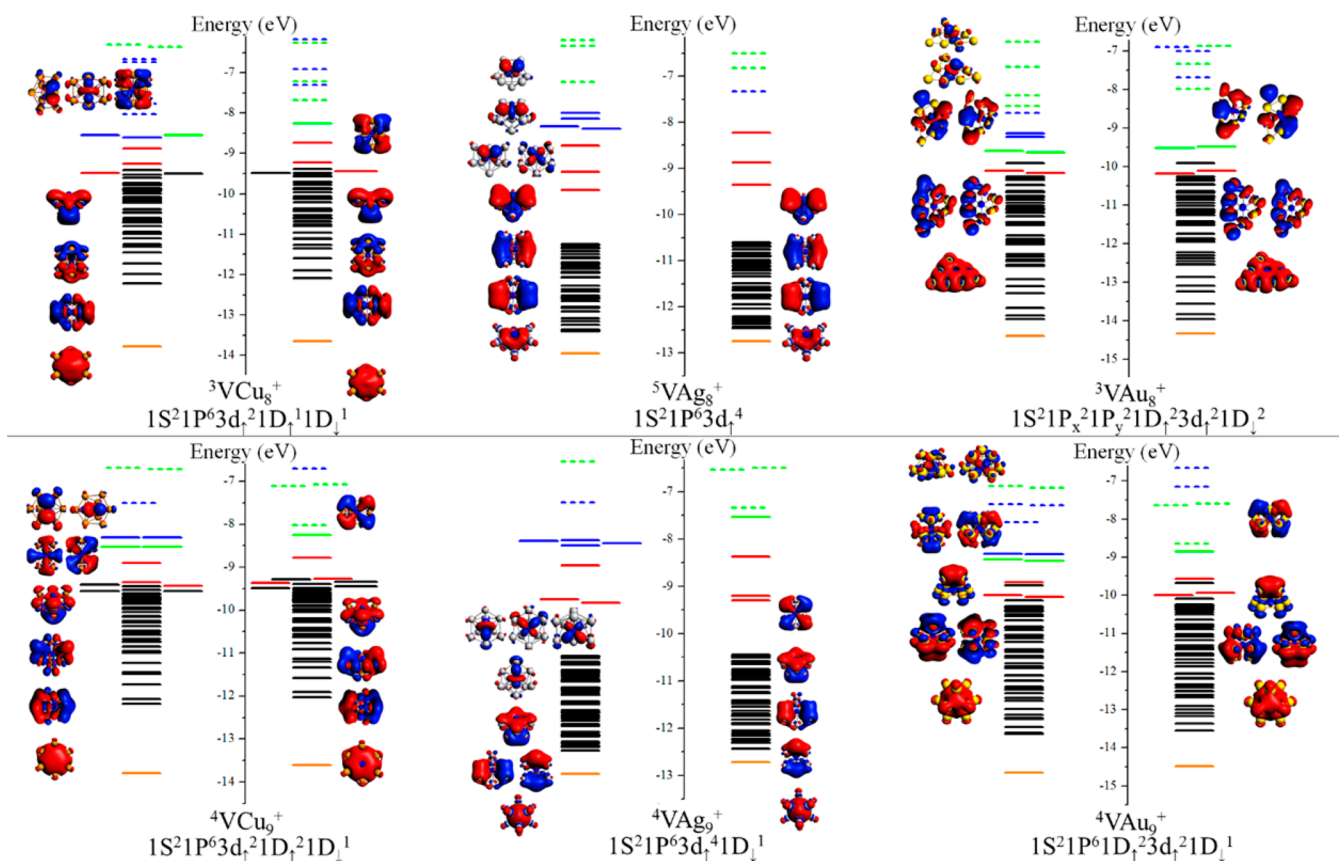


**Figure 6.** Molecular orbital diagrams for  $\text{VCu}_x^+$ ,  $\text{VAg}_x^+$ , and  $\text{VAu}_x^+$  ( $x = 8-9$ ). The filled orange, red, and green lines represent orbitals corresponding to the 1S, 1P, and 1D shells, respectively, and the blue lines represent the localized 3d vanadium orbitals. The dashed lines, the color of which represents the same orbitals as the filled lines, denote the unoccupied orbitals. Pictures of the delocalized orbitals and the localized 3d vanadium orbitals are stacked as they appear in the molecular orbital analysis.

structure of  $^4\text{VAu}_7^+$  is 0.10 eV more stable than the two-dimensional structure, showing that this three-dimensional rearrangement is preferred. This geometric transition allows the  $1\text{P}_z^2$  orbital to drop in energy and become filled, resulting in a closed electronic shell. After this transition,  $\text{VAg}_x^+$  continues to prefer three-dimensional structures, and the 1D cluster orbital eventually begins to fill. However, the gold–vanadium system experiences a transition back to a two-dimensional structure at  $^3\text{VAu}_8^+$ . In  $^3\text{VAu}_8^+$ , the two-dimensional structure is 0.16 eV more stable than the lowest-energy three-dimensional structure. This cluster has nine delocalized electrons; however, only the  $1\text{S}^2$ ,  $1\text{P}_x^2$ , and  $1\text{P}_y^2$  orbitals are filled. Because of its planar-like geometry, the  $1\text{P}_z^2$  orbital is not filled. Again, there is enhanced bonding between the 3d vanadium electrons and the gold, which forms two sets of degenerate 1D cluster orbitals in the spin-majority and spin-minority channels, respectively. This leaves only two localized 3d electrons in the spin-majority channel, which are responsible for a spin magnetic moment of 2. There is a final two- to three-dimensional transition at  $^4\text{VAu}_9^+$ , allowing the  $1\text{P}_z^2$  orbital to be filled. Our calculations reveal there is also partial mixing between the vanadium 3d electrons and the electrons in the gold, providing five electrons in the 3d/1D orbital. This yields an electronic structure of  $1\text{S}^2 1\text{P}^6 1\text{D}_1^2 3\text{d}_1^2 1\text{D}_1^1$ , with three delocalized 1D orbitals, two in the majority and one in the minority spin channel, respectively. An analysis of the molecular orbitals of the  $\text{VCu}_x^+$ ,  $\text{VAg}_x^+$ , and  $\text{VAu}_x^+$  clusters demonstrates that the transition from two- to three-dimensional structures is rooted in the filling of the 1P

cluster orbital shell. In particular, all  $\text{VM}_7^+$  ( $M = \text{Cu}, \text{Ag}, \text{Au}$ ) have the same electronic structure with a  $1\text{S}^2 1\text{P}^6 3\text{d}_1^3$  orbital filling. Because all three 1P cluster orbitals are filled a three-dimensional ground-state structure is found for these clusters, irrespectively of the coin metal.

**3.5. Trends at Larger Sizes in  $\text{VM}_x^+$ ,  $x = 12-14$ ,  $M = \text{Cu}, \text{Ag}, \text{and Au}$ .** A second interesting feature of these clusters is the difference in the HOMO–LUMO gap between  $\text{VCu}_{12}^+$  on one side and  $\text{VAg}_{12}^+$  and  $\text{VAu}_{12}^+$  on the other. The first obvious difference between these clusters is their structure.  $\text{VCu}_{12}^+$  is found to have a  $T_h$  structure that is distorted from an  $I_h$  structure, while  $\text{VAg}_{12}^+$  and  $\text{VAu}_{12}^+$  have cuboctahedral structures. Most interestingly, these different structure motifs can be directly related to the valence of the vanadium atom. To understand this in more detail we plotted the molecular orbitals of these clusters in the top of Figure 7. This figure shows that in  $\text{VCu}_{12}^+$ , the valence of vanadium is 5 with all of the 1D orbitals classified as delocalized, which is confirmed by a Mulliken analysis that shows  $1.02 \mu_B$  on Cu and  $0.98 \mu_B$  on V, as opposed to  $2.57 \mu_B$  and  $2.01 \mu_B$  on V in  $\text{VAg}_{12}^+$  and  $\text{VAu}_{12}^+$ . The stronger localization of the 3d vanadium orbitals in  $\text{VAg}_{12}^+$  and  $\text{VAu}_{12}^+$  introduces in these clusters fourfold rotation axes that pass through the V atom in the center. As a result, a cuboctahedral structure with  $O_h$  symmetry is obtained. On the contrary, the larger delocalization of the 3d vanadium orbitals in  $\text{VCu}_{12}^+$  into the 1D cluster orbitals yields a  $T_h$  structure that can be interpreted as Jahn–Teller distortion of a fictitious icosahedral reference structures due to the partial occupation of

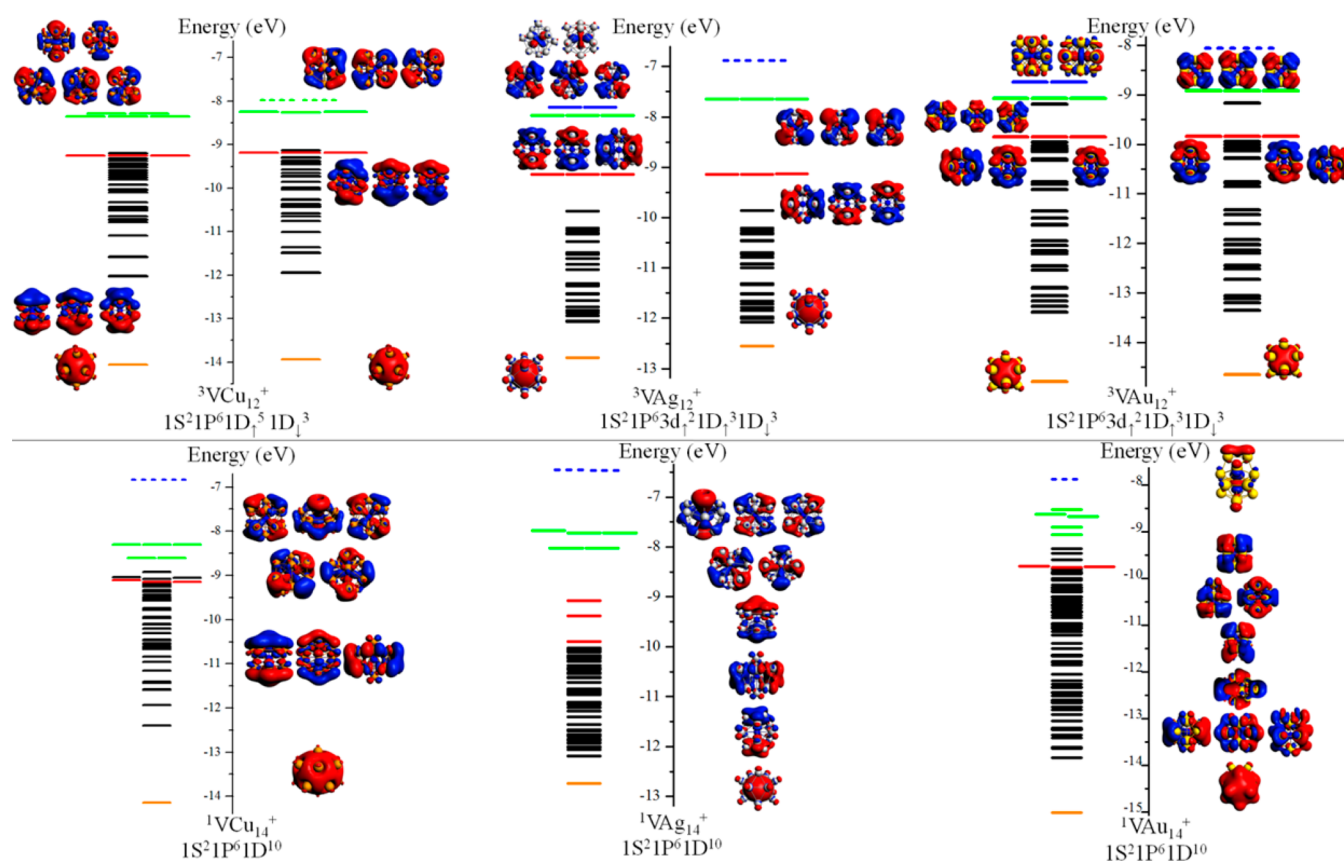


**Figure 7.** Molecular orbital diagrams for  $\text{VCu}_x^+$ ,  $\text{VAg}_x^+$ , and  $\text{VAu}_x^+$  ( $x = 12$  and  $14$ ). The filled orange, red, and green lines represent orbitals corresponding to the 1S, 1P, and 1D shells, respectively, and the blue lines represent the localized 3d vanadium orbitals. The dashed lines, the color of which represents the same orbitals as the filled lines, denote the unoccupied orbitals. Pictures of the delocalized orbitals and the localized 3d vanadium orbitals are stacked as they appear in the molecular orbital analysis.

the 1D shell. Note that the energy ordering of the triple and double degeneracy is inverted in  $T_h$  with respect to the corresponding  $O_h$  splitting in the cuboctahedral  $\text{VAg}_{12}^+$  and  $\text{VAu}_{12}^+$  clusters. That this inverted energy ordering, that is, double degeneracy below triple degeneracy, is not found in  $\text{VCu}_{12}^+$  (see Figure 7 top left) is due to the full occupation of the triple degeneracy and partial occupation of the double degeneracy. This stabilizes the fully occupied triple degeneracy slightly below the partially occupied double degeneracy. As a consequence the HOMO–LUMO gap of the minority-spin channel is only 0.26 eV. Further, the delocalized nature of the orbitals result in a reduced exchange splitting. The corresponding spin-majority channel has a large gap of 1.79 eV consistent with it having a closed shell. In the case of  $\text{VAg}_{12}^+$  and  $\text{VAu}_{12}^+$  the electronic structure of the clusters is  $1S^21P^63d_1^21D_1^31D_1^3$ . Two of the 3d electrons remain localized on the vanadium atom, with 3d occupations of 65% and 57% for  $\text{VAg}_{12}^+$  and  $\text{VAu}_{12}^+$ , respectively. This localization favors a cuboctahedral distortion with low-lying triple degeneracies as shown in Figure 7. For this reason, the exchange splitting is larger than in  $\text{VCu}_{12}^+$ , and the HOMO–LUMO gap increases to relatively large values of 0.76 and 0.69 eV. What is surprising is that at this size, the copper is forming delocalized orbitals with vanadium more easily than gold, while at small sizes gold more readily formed delocalized orbitals with vanadium.

In the case of the spin-quenched  $\text{VCu}_{14}^+$ ,  $\text{VAg}_{14}^+$ , and  $\text{VAu}_{14}^+$ , the clusters all have shell structures of  $1S^21P^61D^{10}$  as shown in the bottom of Figure 7. The vanadium has an effective

valence of 5, and the 3d orbitals are part of fully delocalized orbitals. The 3d V contributions for these orbitals are 15–25% on  $\text{VCu}_{14}^+$ , and  $\text{VAu}_{14}^+$ , and 25–35% for  $\text{VAg}_{14}^+$ .  $\text{VCu}_{14}^+$  and  $\text{VAg}_{14}^+$  have large gaps of 1.46 and 1.21 eV, consistent with their closed electronic shells.  $\text{VAu}_{14}^+$  has a smaller gap of 0.65 eV due to the cluster's unsymmetrical structure. The broadening in the 1D shell is seen in Figure 7, and the LUMO that is constructed from the atomic V  $d_z^2$  orbital is pulled down in energy resulting in a reduced gap. A third unusual case that deserves some consideration is the peak in the HOMO–LUMO gap seen in  $^3\text{VAu}_{10}^+$ , which has 14 valence electrons. The HOMO is a 1D orbital in the minority-spin channel, and the LUMO consists mostly of  $d_z^2$ ,  $d_{xz}$ , and  $d_{xy}$  vanadium states. There are two degenerate 3d vanadium states in the spin-majority channel that are also mostly composed of  $d_z^2$ ,  $d_{xz}$ , and  $d_{yz}$  states. The prolate geometry of  $^3\text{VAu}_{10}^+$  allows the orbitals in the  $xy$  plane to drop in energy, while the  $d_z^2$ ,  $d_{xz}$ , and  $d_{yz}$  states are raised in energy. This results in a significant orbital splitting and a respectable HOMO–LUMO gap of 0.61 eV.

**3.6. General Trends and Peculiarities between Cu, Ag, and Au.** Perhaps the most puzzling result in studying the bonding of  $\text{VCu}_x^+$ ,  $\text{VAg}_x^+$ , and  $\text{VAu}_x^+$  is that at small sizes,  $x = 6$ – $9$ , the 3d orbitals of vanadium bond most readily with gold, while for larger sizes,  $x = 10$ – $13$ , vanadium bonds most readily with copper. Further evidence of this phenomenon is that the multiplicities of the  $\text{VAu}_x^+$  clusters are consistently either less than or the same as those of  $\text{VCu}_x^+$  and  $\text{VAg}_x^+$  from  $x = 3$ – $7$ , while from 8 and larger the multiplicities of  $\text{VAu}_x^+$  and  $\text{VCu}_x^+$

are less than or equal to those of  $\text{VAg}_x^+$ . Because the spin magnetic moment is inversely correlated with the metallic bonding, this suggests that small gold clusters form more metallic bonds, while this is no longer true at larger sizes. Notably, this shift in enhanced bonding with vanadium corresponds to the transition from two- to three-dimensional structures with  $\text{VAu}_x^+$  clusters bonding most readily in two-dimensional structures, and  $\text{VCu}_x^+$  bonding more readily in three-dimensional structures. To understand this variation in electronic structure, occupation of the s and d orbitals of the noble-metal atoms are examined. We have two hypotheses for the differences between the interaction of vanadium with copper, silver, and gold. One hypothesis is that the increased electron affinity of gold causes differences in the bonding. Our second hypothesis is that variations in the sd hybridization within Cu, Ag, and Au result in differences in the bonding. Figure 8 shows the Hirshfeld charges on the vanadium and

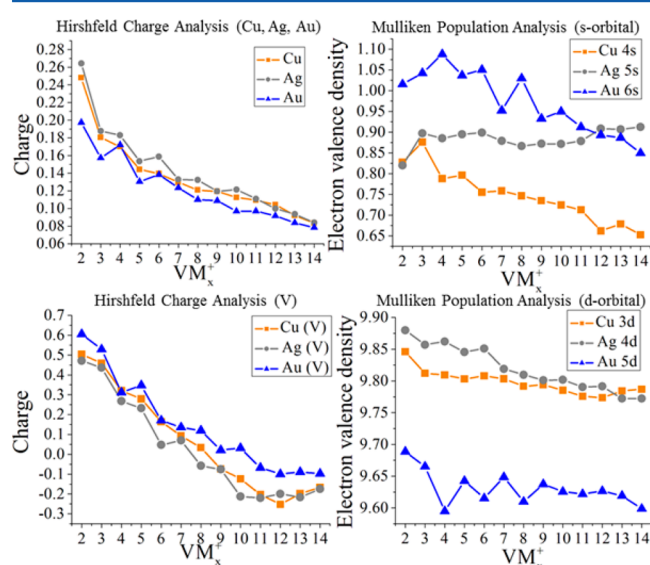


**Figure 8.** Average Hirshfeld charges of Cu, Ag, Au, and V in the  $\text{VCu}_x^+$ ,  $\text{VAg}_x^+$ , and  $\text{VAu}_x^+$  clusters. The Mulliken population of the valence s and d orbitals of Cu, Ag, and Au in the  $\text{VCu}_x^+$ ,  $\text{VAg}_x^+$ , and  $\text{VAu}_x^+$  clusters.

noble-metal atoms. As expected Au is found to be the most negatively charged of the noble metals; however, the difference in charge is quite small, typically in the range of 0.01–0.02  $e^-$  per atom.

Next we examine the s and d occupation of the noble-metal atoms. If the noble-metal atom is behaving as an alkali metal, one would expect that the s occupation would be 1.0, and the d occupation would be 10.0, while hybridization would result in an increase in the s occupation and a decrease in the d occupation. Figure 8 shows that the Ag 5s occupation is 0.90  $e^-$  and that the 4d occupation ranges from 9.90  $e^-$  at small cluster sizes to 9.78 at larger cluster sizes. On the one hand, copper has an even lower 4s occupation, ranging from 0.86 to 0.67  $e^-$ , while the d band is filled with an occupation of 9.85–9.80  $e^-$ . On the other hand, gold exhibits a different trend in orbital occupations with the 6s orbital ranging from 1.08 to 0.86  $e^-$ , with a significantly higher 6s occupation in the two-dimensional clusters. The 5d occupation of Au is significantly lower than for the other noble metals, with an occupation ranging from 9.69 to 9.59  $e^-$ . This increase in 6s occupation and decrease in 5d

occupation is consistent with gold having enhanced 6s-5d hybridization. The two-dimensional  $\text{VAu}_x^+$  clusters, where  $x = 3$ –6 and 8, exhibit peaks in the 6s occupation and valleys in the 5d occupation, consistent with the planar structures having enhanced 6s-5d hybridization. As mentioned earlier, this is due to the relativistic contraction of the 6s orbital and expansion of the 5d orbital resulting in a better than expected spatial overlap between the orbitals.

Also, an even–odd alternation is seen in the V–Au bond distances, while they are not seen in the V–Cu and V–Ag average bond distances. These shortened V–Au bond distances offer further evidence that the localized 3d electrons on the vanadium may successfully couple to the 5d and 6s states of the gold atoms due to superior hybridization and resulting in more contribution to the delocalized orbitals. However, this effect seems to be limited to planar structures, as the hybridization apparently removes charge from the 5d orbitals perpendicular to the planar structure and increases the charge in the plane of the structure. This pronounced sd hybridization is most clear when considering  $^3\text{VAu}_6^+$ , which has 10 valence electrons and an electronic configuration of  $1S^2 1P_x^2 1P_y^2 3d_{\uparrow}^2 1D_{\uparrow}^1 1D_{\downarrow}^1$ . Of these valence electrons, eight are contributing to the delocalized orbitals, and two are localized on the vanadium atom. The interesting point about this cluster is that instead of filling the delocalized  $1P_z^2$  delocalized orbital to be high in energy, and the increased sd hybridization provided by the relativistic quantum effects allows the 1D orbital to partially fill. The atomic contributions reveal that 34% of the 1D delocalized orbital in the majority spin channel is coming from the 3d states on the vanadium, while 66% is coming from the gold. There is also a delocalized 1D orbital in the spin-minority channel that is responsible for the lowered multiplicity of 3. This partial filling occurs at a much smaller size for the gold than the copper and silver vanadium systems, which begin to fill their 1D delocalized orbital at  $^3\text{VCu}_8^+$  and  $^4\text{VAg}_9^+$ , respectively. Once the bonding is both in and out of plane in a three-dimensional structure, the hybridization is reduced in gold. This means that for three-dimensional structures of this size, the copper atoms form metallic bonds with vanadium more readily, while the silver and gold atoms are slightly less likely to form delocalized orbitals than copper. This is confirmed by our molecular orbital plots and the lower alternating spin magnetic moment. The ability to form new metallic bonds with the vanadium are in this larger size range primarily driven by the energy levels of the s and d orbitals of the copper, silver, and gold atoms. Thus, the explanation for the enhanced delocalization in small  $\text{VAu}_x^+$  can be attributed to the relativistic quantum effects experienced by the gold atoms and the subsequent enhanced sd hybridization it provides,<sup>37</sup> while the enhanced delocalization is seen in larger  $\text{VCu}_x^+$  clusters.

#### 4. CONCLUSIONS

The electronic and geometric properties of  $\text{VCu}_x^+$ ,  $\text{VAg}_x^+$ , and  $\text{VAu}_x^+$  clusters have been investigated. Our calculations have shown that the atomic structure of the host cluster plays a significant role in determining the bonding characteristics of a dopant with a localized spin magnetic moment. The metallic bonding between the noble metal and the vanadium atom begins as the 1D delocalized shell begins to form, although the degree of delocalization will depend on the properties of the surrounding atoms. The stability of these bimetallic clusters changes as the delocalized electronic shells are filled, and an

increase in electronic stability is observed. The electronic stability is mostly consistent with a split-shell model in which the valence electrons are partitioned between a delocalized shell and electrons that are localized on the vanadium atom. Which shell is filled depends on whether the geometry of the cluster assumes a two- or three-dimensional structure. To understand this bonding scheme the molecular orbital diagrams of each cluster are considered, and a shell-filling model is applied. The first subshell closure occurs at  $x = 5$ , where the  $1S^2$ ,  $1P_x^2$ , and  $1P_y^2$  orbitals are filled, and there are three localized 3d electrons remaining on the vanadium atom. At  ${}^4VCu_7^+$ ,  ${}^4VAg_7^+$ , and  ${}^4VAu_7^+$  each cluster has eight delocalized electrons, which correspond to a closed electronic shell and enhanced electronic stability. As the clusters grow in size, the 3d states of the vanadium will start to participate in hybridized bonding, eventually fully coupling to the host metal atoms at  ${}^1VCu_{14}^+$ ,  ${}^1VAg_{14}^+$ , and  ${}^1VAu_{14}^+$ . At larger sizes, we observe other local maxima in the HOMO–LUMO gap for  ${}^3VAu_{10}^+$ ,  ${}^3VAg_{12}^+$ , and  ${}^3VAu_{12}^+$ , which can be attributed to their respective geometric configurations. A detailed analysis of the two- to three-dimensional geometric transition of both the gold and silver clusters is provided, and the consequences of this transition are expounded upon by examining the average bond distances of each cluster. The origin of the enhanced delocalization in two-dimensional  $VAu_x^+$  clusters is caused by the enhanced 6s–5d hybridization that occurs because of relativistic effects; however, this hybridization is reduced once the  $VAu_x^+$  clusters form three-dimensional clusters. In three-dimensional clusters, the  $VCu_x^+$  clusters delocalize most readily. Thus, this study has revealed that by changing the composition of a nonmagnetic material that encapsulates a magnetic dopant there are subtle effects that may change the bonding between the magnetic center and the dopant's surroundings. By using different dopants, future studies could be undertaken to see how varying the energy levels of the dopant will affect the bonding scheme of the constituent cluster.

## ■ ASSOCIATED CONTENT

### Supporting Information

The Supporting Information is available free of charge on the ACS Publications website at DOI: 10.1021/acs.jpca.7b01030.

Plots of the average orbital energies, orbital widths, and binding energies (PDF)

## ■ AUTHOR INFORMATION

### Corresponding Authors

\*E-mail: pcalamin@cinvestav.mx. (P.C.)

\*E-mail: snkhanna@vcu.edu. (S.N.K.)

### ORCID

Arthur C. Reber: 0000-0003-1013-331X

Shiv N. Khanna: 0000-0002-9797-1289

### Author Contributions

W.H.B., A.C.R., and S.N.K. contributed to and helped write this manuscript. L.L.S., P.C., and A.M.K. performed and analyzed the deMon2k calculations and contributed to the manuscript. All authors approved the final manuscript. We are also grateful to Prof. P. Lievens for useful discussions.

### Notes

The authors declare no competing financial interest.

## ■ ACKNOWLEDGMENTS

W.H.B., A.C.R., and S.N.K. gratefully acknowledge support by the U.S. Department of Energy (DOE) under Award No. DE-SC0006420. W.H.B. would like to thank Dr. V. Chauhan for his helpful discussions. L.L.S. acknowledges a CONACYT Ph.D. fellowship (397526). Support by CONACYT through Project Nos. CB-252658 and GIC-268251 is gratefully acknowledged by the CINVESTAV groups.

## ■ REFERENCES

- (1) Le, H. T.; Lang, S. M.; Haeck, J. D.; Lievens, P.; Janssens, E. Carbon Monoxide Adsorption on Neutral and Cationic Vanadium Doped Gold Clusters. *Phys. Chem. Chem. Phys.* **2012**, *14*, 9350.
- (2) Claes, P.; Janssens, E.; Ngan, V. T.; Gruene, P.; Lyon, J. T.; Harding, D. J.; Fielicke, A.; Nguyen, M. T.; Lievens, P. Structural Identification of Caged Vanadium Doped Silicon Clusters. *Phys. Rev. Lett.* **2011**, *107*, 173401.
- (3) Medel, V. M.; Reber, A. C.; Chauhan, V.; Sen, P.; Köster, A. M.; Calaminici, P.; Khanna, S. N. Nature of Valence Transition and Spin Moment in  $Ag_nV^+$  Clusters. *J. Am. Chem. Soc.* **2014**, *136*, 8229–8236.
- (4) Espinoza-Quintero, G.; Duckworth, J. C. A.; Myers, W. K.; McGrady, J. E.; Goicoechea, J. M. Synthesis and Characterization of  $[Ru@Ge_{12}]^{3-}$ : An Endohedral 3-Connected Cluster. *J. Am. Chem. Soc.* **2014**, *136*, 1210–1213.
- (5) Abreu, M. B.; Reber, A. C.; Khanna, S. N. Does the 18-Electron Rule Apply to  $CrSi_{12}$ ? *J. Phys. Chem. Lett.* **2014**, *5*, 3492–3496.
- (6) Reveles, J. U.; Clayborne, P. A.; Reber, A. C.; Khanna, S. N.; Pradhan, K.; Sen, P.; Pederson, M. R. Designer Magnetic Superatoms. *Nat. Chem.* **2009**, *1*, 310–315.
- (7) Hölzl, T.; Veldeman, N.; De Haeck, J.; Veszprémi, T.; Lievens, P.; Nguyen, M. T. Growth Mechanism and Chemical Bonding in Scandium-Doped Copper Clusters: Experimental and Theoretical Study in Concert. *Chem. - Eur. J.* **2009**, *15*, 3970–3982.
- (8) Goicoechea, J. M.; McGrady, J. E. On the Structural Landscape in Endohedral Silicon and Germanium Clusters,  $M@Si_{12}$  and  $M@Ge_{12}$ . *Dalton Trans.* **2015**, *44*, 6755–6766.
- (9) Chauhan, V.; Abreu, M. B.; Reber, A. C.; Khanna, S. N. Geometry Controls the Stability of  $FeSi_{14}$ . *Phys. Chem. Chem. Phys.* **2015**, *17*, 15718–157224.
- (10) Knight, W. D.; Clemenger, K.; de Heer, W. A.; Saunders, W. A.; Chou, M. Y.; Cohen, M. L. Electronic Shell Structure and Abundances of Sodium Clusters. *Phys. Rev. Lett.* **1984**, *52*, 2141–2143.
- (11) Brack, M. The Physics of Simple Metal Clusters: Self-Consistent Jellium Model and Semiclassical Approaches. *Rev. Mod. Phys.* **1993**, *65*, 677–732.
- (12) Clemenger, K. Ellipsoidal Shell Structure in Free-Electron Metal Clusters. *Phys. Rev. B: Condens. Matter Mater. Phys.* **1985**, *32*, 1359–1362.
- (13) Li, X.; Wu, H.; Wang, X.-B.; Wang, L.-S. S-P Hybridization and Electron Shell Structures in Aluminum Clusters: A Photoelectron Spectroscopy Study. *Phys. Rev. Lett.* **1998**, *81*, 1909–1912.
- (14) Martin, T. P.; Bergmann, T.; Göhlich, H.; Lange, T. Observation of Electronic Shells and Shells of Atoms in Large Na Clusters. *Chem. Phys. Lett.* **1990**, *172*, 209–213.
- (15) Khanna, S. N.; Jena, P. Atomic Clusters: Building Blocks for a Class of Solids. *Phys. Rev. B: Condens. Matter Mater. Phys.* **1995**, *51*, 13705–13716.
- (16) Reber, A. C.; Khanna, S. N. Superatoms: Electronic and Geometric Effects on Reactivity. *Acc. Chem. Res.* **2017**, *50*, 255–263.
- (17) Reber, A. C.; Khanna, S. N.; Roach, P. J.; Woodward, W. H.; Castleman, A. W. Reactivity of Aluminum Cluster Anions with Water: Origins of Reactivity and Mechanisms for  $H_2$  Release. *J. Phys. Chem. A* **2010**, *114*, 6071–6081.
- (18) Luo, Z.; Reber, A. C.; Jia, M.; Blades, W. H.; Khanna, S. N.; Castleman, A. W. What Determines If a Ligand Activates or Passivates a Superatom Cluster? *Chem. Sci.* **2016**, *7*, 3067–3074.

- (19) Reber, A. C.; Khanna, S. N.; Roach, P. J.; Woodward, W. H.; Castleman, A. W. Spin Accommodation and Reactivity of Aluminum Based Clusters with O<sub>2</sub>. *J. Am. Chem. Soc.* **2007**, *129*, 16098–16101.
- (20) Roach, P. J.; Woodward, W. H.; Castleman, A. W.; Reber, A. C.; Khanna, S. N. Complementary Active Sites Cause Size-Selective Reactivity of Aluminum Cluster Anions with Water. *Science* **2009**, *323*, 492–495.
- (21) Jiang, D.; Whetten, R. L. Magnetic Doping of a Thiolated-Gold Superatom: First-Principles Density Functional Theory Calculations. *Phys. Rev. B: Condens. Matter Mater. Phys.* **2009**, *80*, 115402.
- (22) Walter, M.; Akola, J.; Lopez-Acevedo, O.; Jadzinsky, P. D.; Calero, G.; Ackerson, C. J.; Whetten, R. L.; Grönbeck, H.; Häkkinen, H. A Unified View of Ligand-Protected Gold Clusters as Superatom Complexes. *Proc. Natl. Acad. Sci. U. S. A.* **2008**, *105*, 9157–9162.
- (23) Jug, K.; Zimmermann, B.; Calaminici, P.; Köster, A. M. Structure and Stability of Small Copper Clusters. *J. Chem. Phys.* **2002**, *116*, 4497–4507.
- (24) Jug, K.; Zimmermann, B.; Köster, A. M. Growth Pattern and Bonding of Copper Clusters. *Int. J. Quantum Chem.* **2002**, *90*, 594–602.
- (25) Chen, Z.; Neukermans, S.; Wang, X.; Janssens, E.; Zhou, Z.; Silverans, R. E.; King, R. B.; von Rague Schleyer, P.; Lievens, P. To Achieve Stable Spherical Clusters: General Principles and Experimental Confirmations. *J. Am. Chem. Soc.* **2006**, *128*, 12829–12834.
- (26) Bernhardt, T. M. Gas-Phase Kinetics and Catalytic Reactions of Small Silver and Gold Clusters. *Int. J. Mass Spectrom.* **2005**, *243*, 1–29.
- (27) Medel, V. M.; Reveles, J. U.; Islam, M. F.; Khanna, S. N. Robust Magnetic Moments on Impurities in Metallic Clusters: Localized Magnetic States in Superatoms. *J. Phys. Chem. A* **2013**, *117*, 4297–4303.
- (28) Janssens, E.; Neukermans, S.; Nguyen, H. M. T.; Nguyen, M. T.; Lievens, P. Quenching of the Magnetic Moment of a Transition Metal Dopant in Silver Clusters. *Phys. Rev. Lett.* **2005**, *94*, 113401.
- (29) Janssens, E.; Hou, X. J.; Nguyen, M. T.; Lievens, P. The Geometric, Electronic, and Magnetic Properties of Ag<sub>5</sub>X<sup>+</sup> (X = Sc, Ti, V, Cr, Mn, Fe, Co, and Ni) Clusters. *J. Chem. Phys.* **2006**, *124*, 184319.
- (30) Jin, X.; Espinoza-Quintero, G.; Below, B.; Arcisauskaitė, V.; Goicoechea, J. M.; McGrady, J. E. Structure and Bonding in a Bimetallic Endohedral Cage, [Co<sub>2</sub>@Ge<sub>16</sub>]<sup>2-</sup>. *J. Organomet. Chem.* **2015**, *792*, 149–153.
- (31) Qian, M.; Reber, A. C.; Ugrinov, A.; Chaki, N. K.; Mandal, S.; Saavedra, H. M.; Khanna, S. N.; Sen, A.; Weiss, P. S. Cluster-Assembled Materials: Toward Nanomaterials with Precise Control over Properties. *ACS Nano* **2010**, *4*, 235–240.
- (32) Bergeron, D. E.; Castleman, A. W.; Morisato, T.; Khanna, S. N. Formation of Al<sub>13</sub>I<sup>-</sup>: Evidence for the Superhalogen Character of Al<sub>13</sub>. *Science* **2004**, *304*, 84–87.
- (33) Chauhan, V.; Medel, V. M.; Ulises Reveles, J.; Khanna, S. N.; Sen, P. Shell Magnetism in Transition Metal Doped Calcium Superatom. *Chem. Phys. Lett.* **2012**, *528*, 39–43.
- (34) Chauhan, V.; Sahoo, S.; Khanna, S. N. Ni<sub>9</sub>Te<sub>6</sub>(PEt<sub>3</sub>)<sub>8</sub>C<sub>60</sub> Is a Superatomic Superalkali Superparamagnetic Cluster Assembled Material (S<sup>3</sup>-CAM). *J. Am. Chem. Soc.* **2016**, *138*, 1916–1921.
- (35) Pyykko, P. Relativistic Effects in Structural Chemistry. *Chem. Rev.* **1988**, *88*, 563–594.
- (36) Häkkinen, H.; Landman, U. Gold Clusters Au<sub>N</sub> (2 < N < 10) and Their Anions. *Phys. Rev. B: Condens. Matter Mater. Phys.* **2000**, *62*, R2287–R2290.
- (37) Häkkinen, H.; Moseler, M.; Landman, U. Bonding in Cu, Ag, and Au Clusters: Relativistic Effects, Trends, and Surprises. *Phys. Rev. Lett.* **2002**, *89*, 3.
- (38) Schooss, D.; Weis, P.; Hampe, O.; Kappes, M. M. Determining the Size-Dependent Structure of Ligand-Free Gold-Cluster Ions. *Philos. Trans. R. Soc., A* **2010**, *368*, 1211–1243.
- (39) te Velde, G.; Bickelhaupt, F. M.; Baerends, E. J.; Fonseca Guerra, C.; van Gisbergen, S. J. A.; Snijders, J. G.; Ziegler, T. Chemistry with ADF. *J. Comput. Chem.* **2001**, *22*, 931–967.
- (40) Perdew, J. P.; Burke, K.; Ernzerhof, M. Generalized Gradient Approximation Made Simple. *Phys. Rev. Lett.* **1996**, *77*, 3865–3868.
- (41) Köster, A. M.; Calaminici, P.; Casida, M. E.; Dominguez, V. D.; Flores-Moreno, R.; Gamboa, G. U.; Goursoot, A.; Heine, T.; Ipatov, A.; Janetzko, F.; et al. *deMon2k Program*; deMon developers, 2011.
- (42) Perdew, J. P. Density-Functional Approximation for the Correlation Energy of the Inhomogeneous Electron Gas. *Phys. Rev. B: Condens. Matter Mater. Phys.* **1986**, *33*, 8822–8824.
- (43) Calaminici, P.; Janetzko, F.; Köster, A. M.; Mejia-Olvera, R.; Zuniga-Gutierrez, B. Density Functional Theory Optimized Basis Sets for Gradient Corrected Functionals: 3d Transition Metal Systems. *J. Chem. Phys.* **2007**, *126*, 044108–044108–10.
- (44) Nosé, S. A Unified Formulation of the Constant Temperature Molecular Dynamics Methods. *J. Chem. Phys.* **1984**, *81*, 511–519.
- (45) Hoover, W. G. Canonical Dynamics: Equilibrium Phase-Space Distributions. *Phys. Rev. A: At, Mol, Opt. Phys.* **1985**, *31*, 1695–1697.
- (46) Martyna, G. J.; Klein, M. L.; Tuckerman, M. Nosé–Hoover Chains: The Canonical Ensemble via Continuous Dynamics. *J. Chem. Phys.* **1992**, *97*, 2635–2643.
- (47) Olson, R. M.; Varganov, S.; Gordon, M. S.; Metiu, H.; Chretien, S.; Piecuch, P.; Kowalski, K.; Kucharski, S. A.; Musial, M. Where Does the Planar-to-Nonplanar Turnover Occur in Small Gold Clusters? *J. Am. Chem. Soc.* **2005**, *127*, 1049–1052.
- (48) Gruene, P.; Rayner, D. M.; Redlich, B.; van der Meer, A. F. G.; Lyon, J. T.; Meijer, G.; Fielicke, A. Structures of Neutral Au<sub>7</sub>, Au<sub>19</sub>, and Au<sub>20</sub> Clusters in the Gas Phase. *Science* **2008**, *321*, 674–676.